The structure of the bulk and the (001) surface of V_2O_5. A DFT+U study

2016 Mater. Res. Express 3 085005

(http://iopscience.iop.org/2053-1591/3/8/085005)

Materials Research Express

RECEIVED
21 May 2016

REVISED
13 July 2016

ACCEPTED FOR PUBLICATION
15 July 2016

PUBLISHED
4 August 2016

PAPER

The structure of the bulk and the (001) surface of V_2O_5. A DFT+U study

Víctor A Ranea and Pablo L Dammig Quiña

CCT-La Plata-CONICET. Instituto de Investigaciones Fisico-químicas Teóricas y Aplicadas (INIFTA), Facultad de Ciencias Exactas, Universidad Nacional de La Plata. Calle 64 y diagonal 113 (1900) La Plata, Argentina

E-mail: vranea@inifta.unlp.edu.ar

Keywords: divanadium pentoxide surface, electronic structure, density functional theory, lattice constants, energy gap

Supplementary material for this article is available online

Abstract

GGA (PW91) + U is applied to the calculation of the structure (lattice parameters) and the electronic structure of the V_2O_5 bulk and its (001) surface for different values of U_{eff} used in the literature (0.0, 3.0 and 6.6 eV). Similar surface lattice parameters are calculated for the (001) surface and for the bulk, as well as similar electronic structures. The calculated lattice parameters (*a* and *b* for the surface and *a*, *b* and *c* for the bulk) are in good agreement with experimental results. It seems that there is no strong correlation between the calculated lattice parameters and the value of U_{eff}. The calculated width of the valence band keeps the value of ≈5 eV for the three studied U_{eff}. However, the energy gap between the valence and the conduction bands increases with the value of U_{eff}. $U_{eff} = 3.0$ eV seems to be the most adequate value to describe the energy gap after comparison with experimental results. Electronic density contour plots indicate that for a larger (smaller) U_{eff} the accumulated charge in the V-O(1) bond is overestimated (underestimated). The contour plots (in the *a* direction) show that the charge distribution V-O(3) is less correlated with U_{eff} than the charge distribution V-O(1), whereas charge distribution V-O(2) seems not to be corretaled with U_{eff}. The energy gap between the valence and the conduction bands seems to be strongly related with the charge distribution in the V-O(1) bond. The V-O(1) bond stability seems to be correlated with U_{eff}. However, the stability of the V-O(2) and V-O (3) bonds seems not to be strongly affected by U_{eff}.

1. Introduction

Vanadium oxides are used in the production of chemicals, in catalysis and batteries as well as other uses. The importance of the support in the catalitic properties of the vanadium oxides has also been outlined [1–28]. The bulk V_2O_5 and the V_2O_5(001) surface have been investigated using experimental and theoretical methods [29–34]. Several DFT methodologies have been applied to the optimization of the lattice parameters [30, 33–42]. Those calculations have been performed within the DFT framework with periodic boundary conditions. The *a* and *b* (*in plane*) lattice parameters are in good agreement with the experimental values in general [32]. The van der Waals interactions were included in some of the works in order to take into account the weak interactions between layers that gives a better agreement with the *c* lattice parameter (perpendicular to the (001) surface).

Generalized gradient approach (GGA) and GGA+U methods were applied in order to calculate the energy for a number of oxidation reactions of 3*d* transition metal oxides [43]. In the article, the authors found that the use of the GGA+U method makes possible to address the correlation effects in the 3*d* transition metal oxides. The calculated oxidation energies agree well with experimental information for the values given to U_{eff}. They found that for many of the metal oxides they studied, the U_{eff} value that corrects the oxidation energy also improves the magnetic moments and the band gaps. In particular, for V_2O_5 the calculated band gap is 1.6 and 2.1eV using GGA and GGA+U methods, respectively; whereas 2.0 and 2.2 eV are experimental values according to references [44] and [45], respectively. They found a value of $U_{eff} \approx 3$ eV for a few vandium oxides [43].

The value $U_{eff} = 3$ eV [46] was also used to describe the surface metal-insulator transition of a V_2O_5(001) single crystal [47]. In the experimental study a reversible metal to insulator transition occurs at 350–400 K. Density functional theory and Monte Carlo simulations support the experimental results on the basis of anisotropic growth of vanadyl oxygen (V = O) vacancies at the surface.

GGA and GGA+U methods were also applied in a study about structural, electronic and magnetic properties of V_2O_{5-x} [39]. In the study the authors set U = 3 eV and J = 0.9 eV ($U_{eff} = 2.1$ eV) in their calculations on the V_2O_5 with oxygen vacancies. They found the effect of the on-site Coulomb interaction of the V 3*d* electrons on the magnetic properties is not strong per oxygen vacancy.

Recently, the selective oxidation of propane on the fully oxidized V_2O_5(001) surface was studied using PBE +U [48]. In the work the on-site repulsion parameter U_{eff} was set to 6.6 eV for V on the vanadium oxide catalyst with and without titania support. It was found that the monocoordinated oxygen is the most active site on the surface without and with the titania support. The bridging oxygen is more selective in the propane deshydrogenation.

GGA+U and experimental methods [49] were used in the study of the electronic structure of V_2O_5, reduced V_2O_{5-x} and sodium intercalated NaV_2O_5. In that study, the effective Hubbard U-J = 5.89 eV was added for the vanadium 3*d*-states. They found that theoretical calculations and experimental results are in good agreement. Local density approximation (LDA+U), with similar value of U_{eff}, was applied to α-NaV_2O_5 [50]. This approach has produced the insulating antiferromagnetic solution with an energy gap of 2.7 eV and a magnetic moment of 0.97 μB only on one type of vanadium atom. The authors indicated that their results were in satisfactory agreement with experimental results.

In the present manuscript, a number of calculations were performed in order to calculate the V_2O_5(001) surface lattice parameters, *a* and *b*, and the V_2O_5 bulk lattice parameters (*a*, *b* and *c*), for different U_{eff} values: 0.0, 3.0 and 6.6 eV. The value $U_{eff} = 0.0$ eV is chosen because is the plain DFT framework, PW91 in this manuscript. The value $U_{eff} = 3.0$ eV is important because it seems to predict, or be in agreement with, the experimental energy gap between the valence and the conduction bands for the V_2O_5 bulk. The value $U_{eff} = 6.6$ eV is the maximum value used in the literature (to our knowledge). One of the aims of this manuscript is to learn if one of these values of U_{eff} is the most adequate for describing the *a* and *b* lattice parameters after comparison with experimental results. It seems that none of them give a better description of the lattice parameters or, in other words, there is no strong correlation between the value of U_{eff} and the calculated surface lattice parameters *a* and *b*. A comparison of the orbital energies of the V_2O_5(001) optimized surface is given for different U_{eff} values. Total and projected density of states are calculated within the GGA (PW91) + U formalism and compared for $U_{eff} = 0.0$, 3.0 and 6.6 eV. Despite the calculated lattice parameters, for the bulk and for the (001) surface, are not correlated with the election of U_{eff}, the election of $U_{eff} = 3.0$ eV seems to be the best one to describe the energy gap between the valence and the conduction bands after comparison with experimental results. After this conclusion, the stability of the V-O(1) bond is underestimated and overestimated for $U_{eff} = 0.0$ and 6.6 eV, respectively. However, the stability of the V-O(2) and V-O(3) bonds is not strongly correlated with U_{eff}. It seems that the energy gap between the valence and the conduction bands is strongly correlated with the charge density distribution in the V-O(1) bond. Density charge distribution plots show there is an under and overestimation of the charge accumulation between the V and O(1) atoms using U_{eff} 0.0 and 6.6 eV, respectively. The strength of the bonds, according to charge accumulation, is V-O(1) bond stronger than V-O(2) bond and V-O(2) bond stronger than O(3) bond.

2. Methodology

First-principles total energy calculations were performed using density functional theory (DFT) as implemented in the Vienna Ab initio Simulation Package (VASP) [51, 52] to investigate the structure and the electronic structure of the V_2O_5(001) surface and the V_2O_5 bulk. The Kohn-Sham equations were solved using the projector augmented wave (PAW) approach for describing electronic core states [53, 54] and a plane-wave basis set including plane waves up to 400 eV. Electron exchange and correlation energies were calculated within the generalized gradient approximation (GGA) in the Perdew-Wang (PW91) form [55]. For U_{eff} equals to 3.0 and 6.6 eV, the values 4 and 7.6 eV were given to U, respectively; in both cases, J = 1 eV. U and J were not included in the $U_{eff} = 0$ (GGA) calculations. The Dudarev *et al* approach is used [56] and, U and J are given to Vanadium only. In this approach only U-J(=U_{eff}) is meaningful.

Each system (the V_2O_5(001) surface and vacuum, and the bulk) were modeled by a different orthorhombic supercell. In the case of the surface, the lattice parameters *a* and *b* were calculated following the iterative procedure described here, for the U_{eff} values. First step, keep the value of the *b* lattice parameter fixed and perform calculations to optimize the geometry of the system for different values of the *a* lattice parameter until the minimum energy is found. Second step, keep the *a* lattice parameter fixed at the value found in the first step,

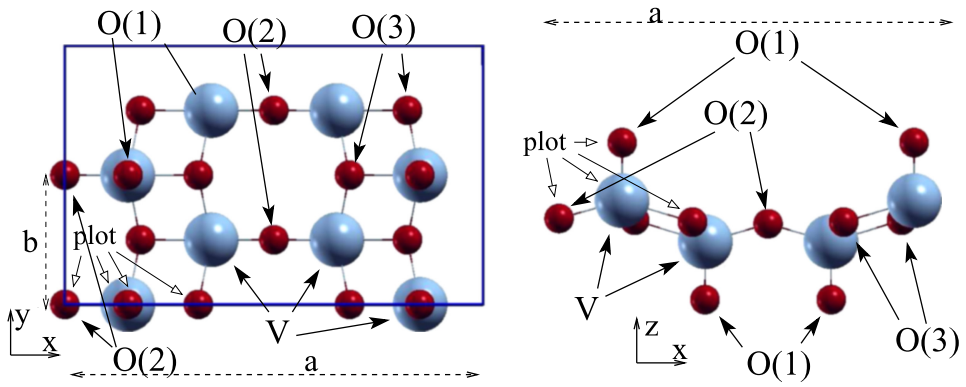

Figure 1. Clean V_2O_5(001) surface cell used in the present manuscript. The *a* and *b* lattice parameters of the surface cell are marked. A (1 × 2) surface is marked with the rectangle. Vanadium (V, light blue balls) and oxygen atoms (O(1), O(2) and O(3), red balls) are marked. The *x*, *y* and *z* axes are also indicated. The V, O(1), O(2) and O(3) atoms used in figure 6 for charge density contour plots are marked with *plot* and white arrows. The figure has been made with the xcrysden program [63].

Table 1. Calculated *a* and *b* lattice parameters (Å) for the (001) surface and *a*, *b* and *c* lattice parameters for the bulk structure of the V_2O_5. Also shown previous results from the literature for the bulk structure.

	$U_{eff} = 0.0$		$U_{eff} = 3.0$		$U_{eff} = 6.6$		Results from references				
	layer	bulk	layer	bulk	layer	bulk	[29]	[32]	[26]	[38]	[64]
a	11.41	11.60	11.34	11.56	11.36	11.58	11.4959(95)	11.512	11.512	11.532	11.519
b	3.57	3.57	3.63	3.63	3.69	3.71	3.5510(51)	3.564	3.564	3.600	3.564
c		4.39		4.63		4.66	4.3569(25)	4.364	4.368	4.401	4.373

and perform geometry optimizations for different values of the *b* lattice parameter until the minimum energy is found. Third step, keep the *b* lattice parameter fixed at the value found in the second step, and perform geometry optimizations for different values of the *a* lattice parameter until the minimum energy is found. Continue with this iterative procedure until the configuration of minimum energy is found for both, *a* and *b* lattice parameters. Similar iterative procedure was used to find *a*, *b* and *c* lattice parameters for the bulk for every value of the chosen U_{eff}. A few articles, exchange the lattice constants *b* and *c* and the (001) plane is named (010) plane [34]. The surface was modeled by a monolayer thick slab separated by more than 15 Å vacuum region to avoid interactions between slabs due to periodic boundary conditions in the perpendicular to the surface direction. All the atoms of the surface and of the bulk, were allowed to relax freely according to the calculated forces applied on them. Atomic relaxations are considered converged when the forces on the ions are less than 0.01eV/Å. The first Brillouin zone of the supercell was sampled with a (4 × 10 × 1) Γ centered mesh resulting in 22 irreducible **k**-points for the surface calculations and with a (1 × 3 × 3) Γ centered mesh for the bulk case. The energies of the DOS calculations have been shifted to have the parameter E-fermi in 0.0 eV.

3. Results and discussion

3.1. Structure of the divanadium pentoxide, bulk and (001) surface lattice parameters

The structure of the divanadium pentoxide (V_2O_5) has been investigated using different experimental and theoretical techniques [29, 30]. It has been described in previous articles ([31, 32, 34, 57] and references within) and a short description is given here. Divanadium pentoxide has an orthorhombic structure with lattice parameters *a*, *b* and *c*. The divanadium pentoxide bulk structure is made of layers that are perpendicular to the *c* axis, each layer is made of VO_6 octahedra [31] at two levels. The layers are linked vertically by corners, in the [001] direction (*c* axis). Figure 1 shows the surface supercell used in this manuscript, lattice parameters *a* and *b* are marked. The reported lattice parameters seem to be in agreement among them and are listed in the table 1 together with the ones calculated in the present work for the surface and the bulk. The weak bond between layers is considered as van der Waals bond, and it is responsible for layer binding [30]. In every layer, oxygen atoms can be classified into three types according to the number of vanadium atoms to which they are bound: O(1) terminal oxygen atoms or vanadyl oxygens, bound to one vanadium atom, O(2) coordinated to two vanadium atoms and O(3) coordinated to three vanadium atoms. Vanadium atoms are linked to five oxygen atoms (one O(1), one O(2) and three O(3)) within the layer and weakly linked the one O(1) of the next layer (van der Waals

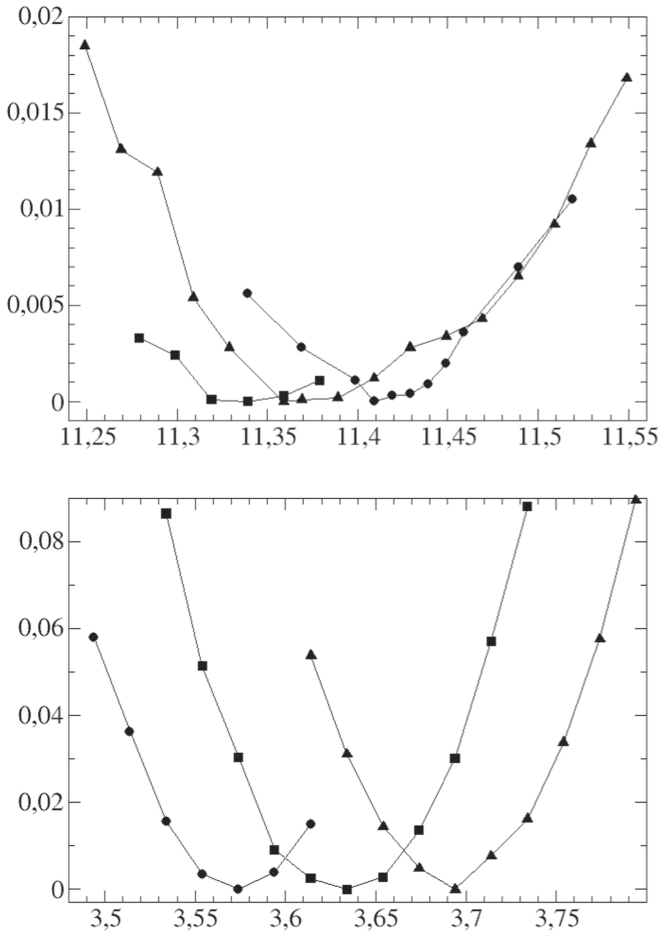

Figure 2. Last step in the calculation of the lattice parameters *a* (top) and b (bottom) for different values of U_{eff}: 0.0 (circles), 3.0 (squares) and 6.6 (triangles) eV. The calculated values for the lattice parameter *a* are 11.41, 11.34 and 11.36 Å using U_{eff} 0.0, 3.0 and 6.6 eV, respectively. The calculated values for the lattice parameter *b* are 3.57, 3.63 and 3.69 Å using U_{eff} 0.0, 3.0 and 6.6 eV, respectively. Energy (eV) in the vertical axis and lattice parameters in the horizontal axis (Å).

interaction). In this way a VO_6 octahedrom is formed [57]. The (001) face is the most stable single-crystal surface [31, 58]. Experimental and theoretical studies have shown that the (001) surface has very similar physical properties and stability as the bulk crystal [34, 35, 48, 59–61]. Therefore, in this manuscript the substrate is modeled by a single slab that can be considered as a realistic model of the V_2O_5(001) surface. Results obtained in this manuscript support this statement. The calculated single layer electronic structure is similar to the calculated electronic structure for the bulk, for the three values of U_{eff} used in this work. For the surface and for the bulk, a number of calculations were performed for different values of the lattice parameters *a*, *b* and *c* in order to calculate the values that minimize the energy, for every U_{eff}. Figure 2 shows the calculated relative energy of the V_2O_5(001) surface versus values given to the lattice parameters *a* (top) and *b* (bottom) around the minimum energy (in every case). The calculated values for the lattice parameter *a* are 11.41, 11.34 and 11.36 Å using U_{eff} 0.0, 3.0 and 6.6 eV, respectively. The calculated values for the lattice parameter *b* are 3.57, 3.63 and 3.69 Å using U_{eff} 0.0, 3.0 and 6.6 eV, respectively. In the upper (bottom) part of figure 2, different values are given to the lattice parameter *a* (*b*) for a fixed value of the lattice parameter *b* (*a*). Figure 2 shows that the energy of the surface is minimum for the values of the lattice parameters recently mentioned. For every U_{eff}, the energy differences shown in figure 2 are very small and so the curves around every minimum are shallow. This would show some sort of flexibility in the *ab plane*, mainly in the *a* direction. The top panel of figure 2 shows for $U_{eff} = 3.0$ eV that the *a* lattice constant could be between ≈12.28 and ≈12.38 Å within 4 meV of energy. The layer also show some flexibility in the *c* direction ([001] direction). Using $U_{eff} = 3.0$ eV there is a displacement in the [001] direction of the two O(2) atoms of the unit cell of about 0.03 Å with an energy difference of 2 meV. The lattice parameters *a* and *b* seem not to be correlated with the value of U_{eff}. In other words, the calculated lattice parameters *a* and *b* seem to be independent of the value assigned to U_{eff}, within the scope of this manuscript. The comparisons among the *a* values and among the *b* values with the experimental values (see table 1) shows that it is not possible to determine which value of U_{eff} is the most adequate to model the surface or they are all good enough to model

Table 2. Calculated vanadium—oxygen bond lengths (Å) for the V_2O_5(001) surface (left) and for the V_2O_5 bulk (right). There are two O(3)-V bond lengths, the longest (shortest) is near the direction of the *a* (*b*) lattice parameter, see figure 1. Results from the literature are included for comparison.

	$U_{eff} = 0.0$	$U_{eff} = 3.0$	$U_{eff} = 6.6$	[49]	[33]	[32]
O(1)	1.60 / 1.61	1.60 / 1.60	1.58 / 1.59	1.576	1.60	1.59
O(2)	1.79 / 1.79	1.80 / 1.80	1.82 / 1.82	1.778	1.79	1.80
O(3)	1.89 / 1.88	1.92 / 1.91	1.94 / 1.94	1.878	1.89	1.90
	2.02 / 2.04	2.00 / 2.03	2.00 / 2.01	2.017	2.04	2.05

the V_2O_5(001) surface. Similar conclusions are valid for the *a* and *b* lattice parameters for the bulk calculations. However, for every U_{eff}, the *a* and *b* lattice parameters calculated for the layer are slightly shorter than the experimental results, whereas the ones calculated for the bulk are a bit longer. The calculated *a* lattice parameter for the bulk is ≈0.2 Å longer than the calculated for the (001) surface. In the case of the *c* lattice parameter of the bulk calculations, the van der Waals interactions are not taken into account, and the separation between layers is a bit overestimated.

The optimized V-O bond lengths of the V_2O_5(001) surface and of the V_2O_5 bulk are in good agreement between them and are not correlated with the values of U_{eff} used in this manuscript ($U_{eff} = 0.0$, 3.0 and 6.6 eV), as shown in table 2. Also, there is good agreement when optimized V-O bond lengths are compared with previous published results.

3.2. Electronic structure of the divanadium pentoxide, bulk and (001) surface

Calculations of the electronic structure of the V_2O_5(001) surface and of the V_2O_5 bulk were performed with the calculated lattice parameters for every U_{eff} value.

Total DOS, valence band and energy gap. Calculated total density of states (DOS) of the bulk V_2O_5 and of its (001) surface for different values of U_{eff} are shown on figure 3: $U_{eff} = 0.0$, 3.0 and 6.6 eV from the top. Negative energy values and DOS larger than zero refer to the valence band and positive energy values and DOS larger than zero refer to the conduction band. In the case of the surface, at first glance, the valence band shows a large maximum around its middle region for $U_{eff} = 0.0$ eV. Altough the maximum is smaller for $U_{eff} = 3.0$ eV, the general shape of the valence band is similar to the previous case (continuous lines). This maximum is due to the O(1)p_z and Vd_{z^2} orbitals and it is not so strong in the cases of bulk calculations (dashed lines). For $U_{eff} = 6.6$ eV, the general shape seems to be similar to the previous cases, but the maximum is not in the middle of the valence band but there is one near the bottom of the band (low energies) and another one near the top (high energies). The width of the valence band seems not to be correlated with the value of U_{eff}, for the surface and for the bulk. For the surface is about 4.87, 4.75 and 4.78 eV for $U_{eff} = 0.0$, 3.0 and 6.6 eV, respectively, (in agreement with previous DFT results [33]) whereas the calculated valence band for bulk are less than 0.2 eV wider than those values. The calculated width of the valence band is then, not correlated with the value of the U_{eff}, at least the ones used in the present work. A wider valence band of 5.5 eV was calculated using a different computational set up in references [34] and [41] for LDA and GGA ($U_{eff} = 0$ eV). Also, the angle resolved He-II ultraviolet photoemission spectrum of a V_2O_5(001) surface sample taken at normal incidence shows a wider range of about 6 eV [41, 62].

For bulk and surface, at higher energies, the calculated energy gap between the valence and the conduction bands depends on the value given to U_{eff} as well as the width and shape of the conduction band. In the case of the surface, the calculated energy gaps are 1.81, 2.19 and 2.95 eV for $U_{eff} = 0.0$, 3.0 and 6.6 eV, respectively. In comparison, the energy gaps calculated for the bulk are between 0.1 and 0.2 eV smaller as shown in figure 3. Comparison with experimental values (2.0 and 2.2 eV according to references [44] and [45], respectively) shows an underestimation and overestimation of the energy gap using $U_{eff} = 0.0$ and 6.6 eV. Also, the energy gap calculated with the present computational set up is a bit higher than the one calculated in reference [43]. However, $U_{eff} = 3.0$ eV seems to be, or seems to be near, the correct value in order to describe the energy gap.

The calculated widths of the conduction band are 2.34, 2.28 and 1.47 eV, for $U_{eff} = 0.0$, 3.0 and 6.6 eV, respectively, for the surface and the bulk.

PDOS, O(1). There is an energy shift for the p_z atom projected PDOS when the U_{eff} changes values. The energy shift is about 0.4 eV when U_{eff} changes values from 0.0 to 3.0 eV and is about 1.4 eV when U_{eff} changes values from 0.0 to 6.6 eV, figure 4. The *z* axis is the direction of the V-O(1) bond, figure 1. The atom projected PDOS of the O(1) contributes mainly to the middle and top parts of the valence band. The main peak for $U_{eff} = 0.0$ and 3.0 eV, see figure 3, seems to be due to a large contribution of the O(1)p_z orbital (also, due to the Vd_{z^2}). There is no strong change in the p_x and p_y atom projected PDOS of the O(1), only a shift smaller than 0.2 eV of a few peaks to lower energies when the U_{eff} takes values 0.0, 3.0 and 6.6 eV, complementary material

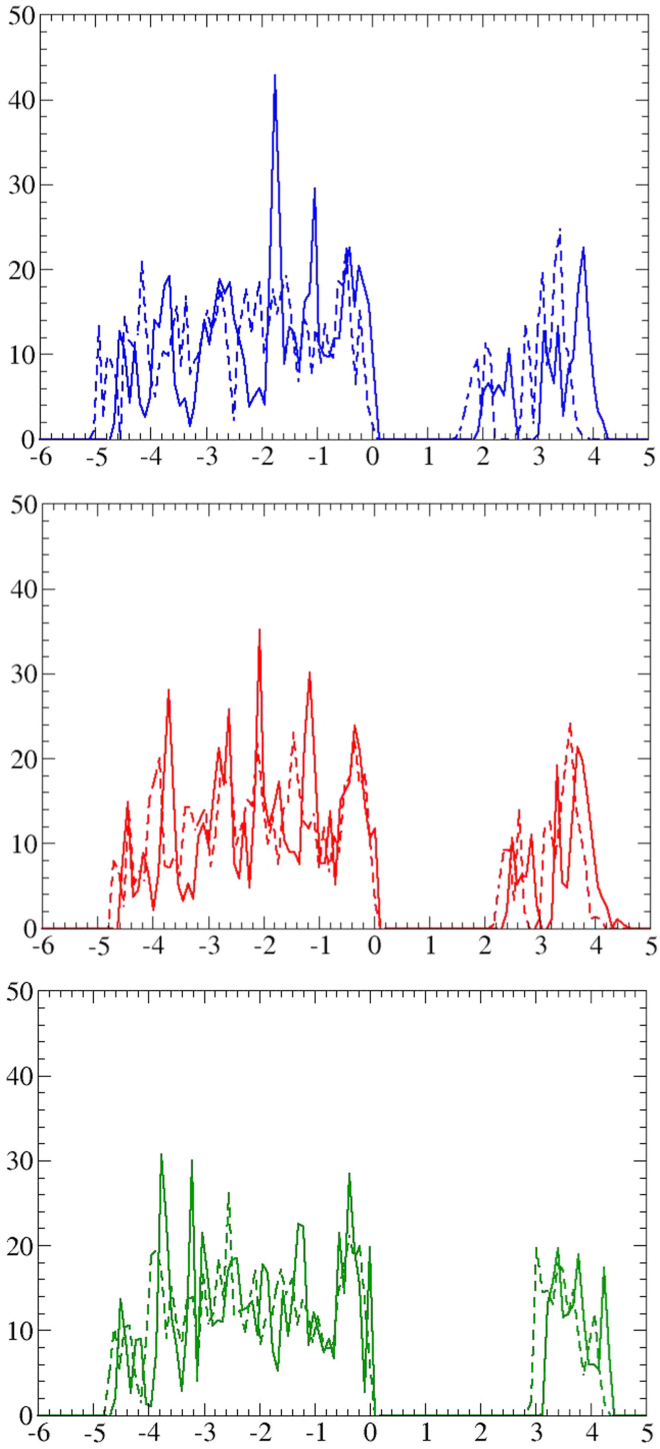

Figure 3. Calculated density of states (DOS) of the clean V_2O_5(001) surface and of the V_2O_5 bulk, for different values of U_{eff}: 0.0 eV (top panel, blue continuous and dashed lines), 3.0 eV (middle panel, red continuous and dashed lines) and 6.6 eV (green continuous and dashed lines). DOS in the vertical axis (number of states/unit cell), energy (eV) in the horizontal axis.

(*x* and *y* axes are shown in figure 1). Similar characteristics in the case of the bulk for the p_z atom projected PDOS, figure 5, but the valence band is much less neat than in the surface case, for the p_x and p_y atom projected PDOS (complementary material).

PDOS, O(2). In the case of the surface, there is an important contibution of the p_x orbital of the O(2) near the bottom of the valence band, figure 4. It should be notice that the *x* direction is (near) the V-O(2)-V bonds direction as shown in figure 1. The p_y and p_z main contributions are in the middle and top parts of the valence band (complementary material). In the *y* direction, the peak in the middle of the valence band seems to shift slightly towards higher energies when U_{eff} takes the values 0.0, 3.0 and 6.6 eV. This shift is stronger in the case of the bulk (complementary material). The contribution of the p_z peak to the middle of the valence band seems to

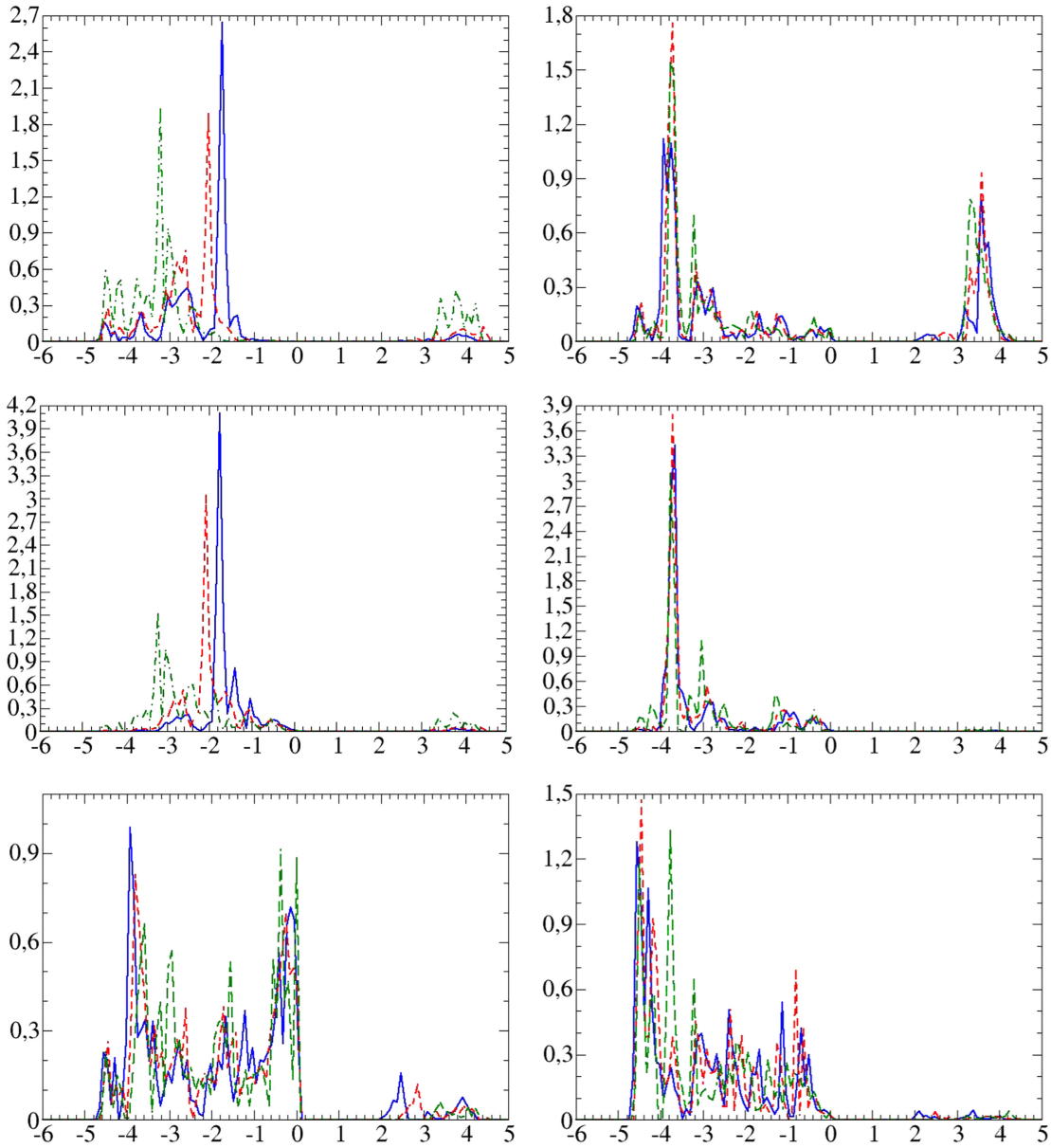

Figure 4. Calculated atomic projected density of states (DOS) of the clean $V_2O_5(001)$ surface: (top panel) Vd_{z^2} (left) and V$d_{x^2-y^2}$ (right), (middle panel) O(1)p_z (left) and O(2)p_x (right), (bottom panel) O(3)p_x (left) and O(3)p_y (right). Different values of U_{eff} are shown: 0.0 eV (blue continuous line), 3.0 eV (red dashed line) and 6.6 eV (green dot-dashed line). DOS in the vertical axis (number of states/unit cell), energy (eV) in the horizontal axis.

decrease for $U_{eff} = 6.6$ eV but there are not energy shift of the peaks. The peak around −3.8 eV in the three total DOS plot shown in figure 3 seem to be due to the O(2)p_x orbital mainly, with contributions of V$d_{x^2-y^2}$ and O(3) p_x orbitals. In the case fo the bulk, there is a very little shift of the main peak towards higher energies when using $U_{eff} = 0.0$, 3.0 and 6.6 eV, figure 5 for the p_x contribution.

PDOS, O(3). For surface and bulk, figures 4 and 5 show the p_x atom projected PDOS contributes to the top and near the bottom of the valence band to the total DOS. There is a shift of ≈0.3 eV near the bottom of the valence band when U_{eff} increases from 0.0 to 3.0 and to 6.6 eV. The contribution to the upper part of the valence band is not correlated with U_{eff}. The O(3)p_y atom projected PDOS contributes mainly to the bottom of the valence band and there is, also, a shift of ≈0.2 eV upward in energy, when U_{eff} increases from 0.0 to 3.0 and to 6.6 eV. Near the *x* direction there is one V-O(3) bond, whereas near the *y* direction there are two V-O(3) bonds. For surface and bulk, the p_z atom projected PDOS contributes mainly to the top of the valence band (complementary materials), however, there is a contribution to the total DOS of the middle region in the case of the surface. There is a small projection of the V-O(3) bonds in the *z* direction.

PDOS, V. The contribution of the d_z^2 orbital is in the middle of the valence band and is the most important among the vanadium *d* orbitals to the total DOS for the bulk and the surface, figures 4 and 5. In the case of the

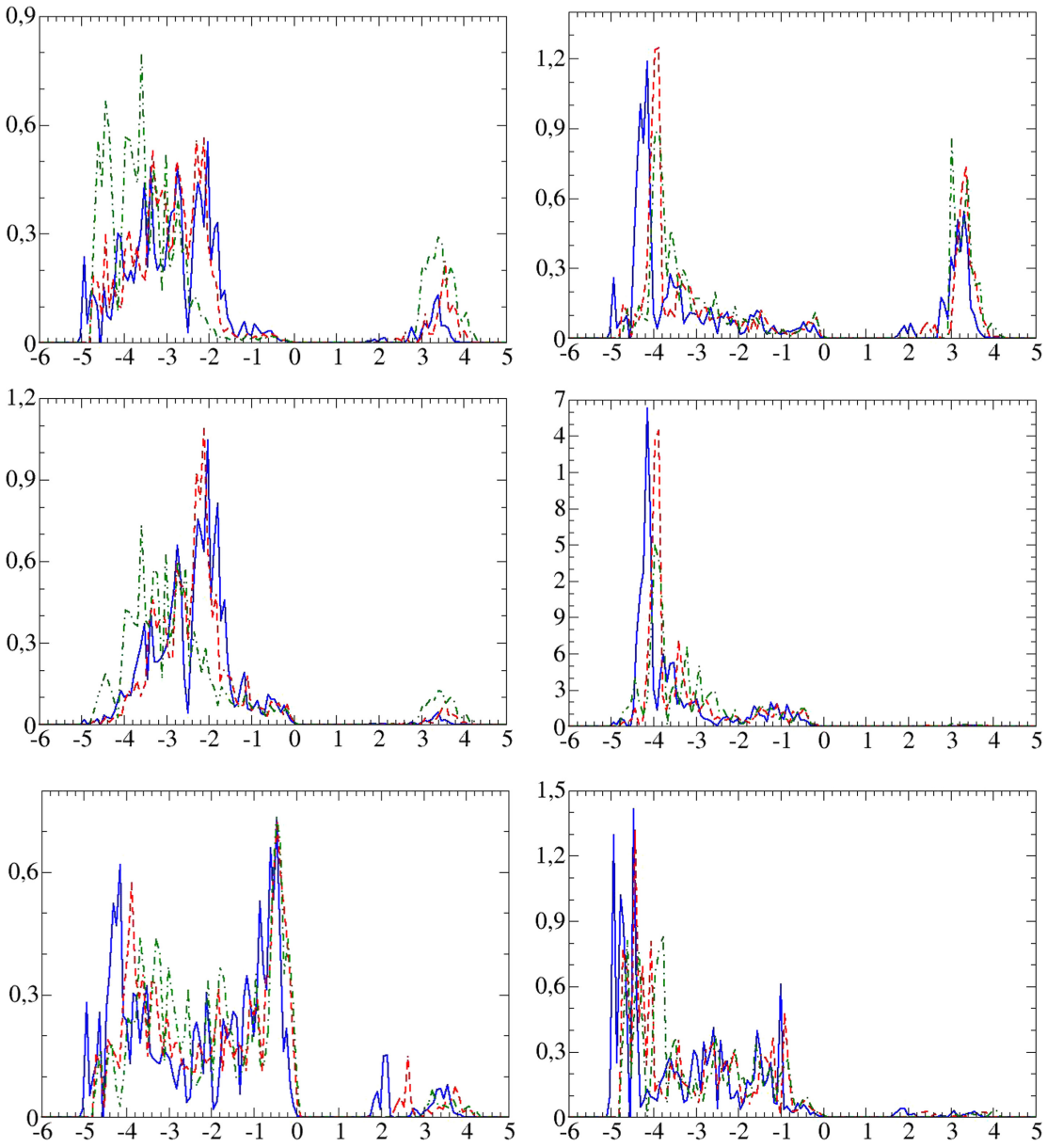

Figure 5. Calculated atomic projected density of states (DOS) of the buk V_2O_5: (top panel) Vd_{z^2} (left) and V$d_{x^2-y^2}$ (right), (middle panel) O(1)p_z (left) and O(2)p_x (right), (bottom panel) O(3)p_x (left) and O(3)p_y (right). Different values of U_{eff} are shown: 0.0 eV (blue continuous line), 3.0 eV (red dashed line) and 6.6 eV (green dot-dashed line). DOS in the vertical axis (number of states/unit cell), energy (eV) in the horizontal axis.

surface, the atom projected PDOS shows a main peak that shift to lower energies, −1.8, −2.1 and −3.3 eV as the value of U_{eff} increases 0.0, 3.0 and 6.6 eV, respectively. The z direction is the V-O(1) bond direction, figure 1. There is not a main peak in the case of the bulk, but the general behaviour is that the peaks shift to lower energies as the U_{eff} increases. Figures 4 and 5 show some contibution of the $d_{x^2-y^2}$ orbital to the total DOS in the lower half of the valence band, for any of the values of the U_{eff} considered, for surface and bulk. The V-O(2) and V-O (3) bonds are mainly in the x and y directions with little projection in the z direction. There is very little contribution of the d_{xy}, d_{xz} and d_{zy} orbitals to the total DOS for bulk and surface (complementary materials).

V-O(1) bond. Figure 4 shows, for the surface, a comparison between the atomic projected PDOS of the O(1) p_z and Vd_{z^2} orbitals for the values of U_{eff} studied here. There are common features between the above mentioned orbitals. For $U_{eff} = 0.0$ eV (blue continuous line), there is a peak around −1.8 eV and a small band between −2.2 and −3.2 eV. For $U_{eff} = 3.0$ eV (red dashed line), there is a main peak around −2.1 eV and also a small band between −2.4 and −3.2 eV. And for $U_{eff} = 6.6$ eV (green dot-dashed line), there is a peak around −3.3 eV and a main small band between −3.4 and −4.6 eV. The comparison seems to indicate that the common features shift the energy values to the lower part of the valence band. Probably this indicates that the V-O(1) bond is more stable when the U_{eff} increases its values: 0.0, 3.0 and 6.6 eV. If the 'true' value of U_{eff} is around

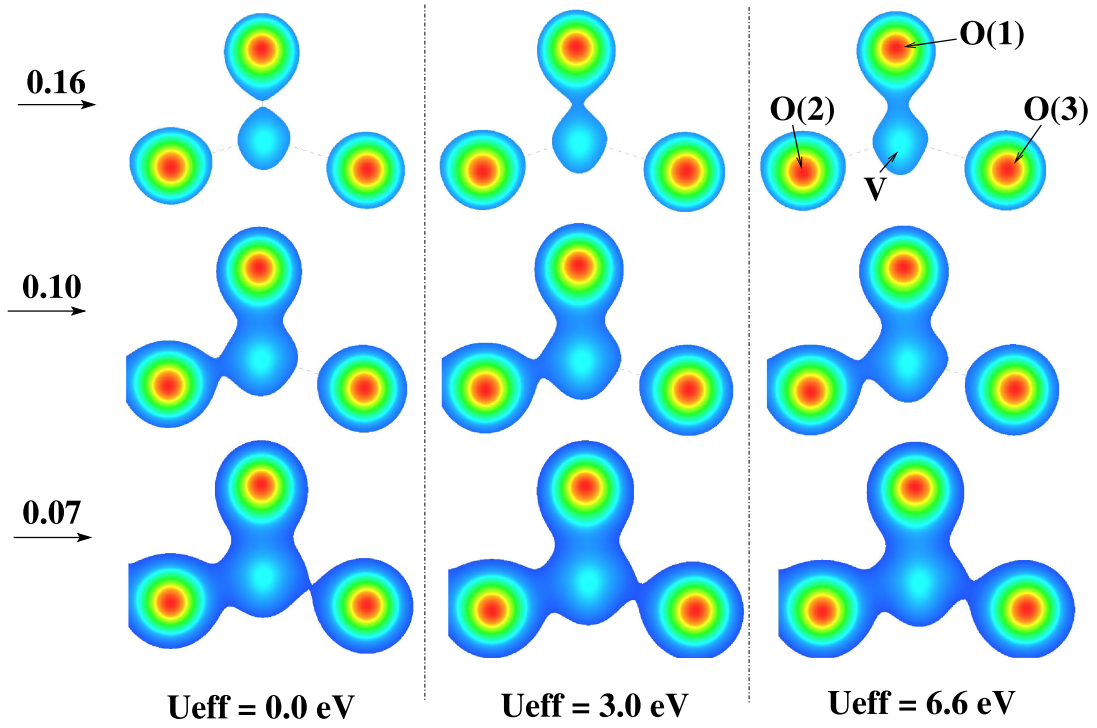

Figure 6. Calculated charge density contour plots (e/Bohr^3) for the three U_{eff} values: 0.0, 3.0 and 6.6 eV (left, central and right panels). On the left, the values of the minimum charge density ploted, the maximum charge correspond to 1.19 e Bohr^{-3}, where the oxygen atoms are (red, on line version). The V, O(1), O(2) and O(3) atoms used are marked on figure 1 with *plot* and white arrows. The figure has been made with the vesta program [65].

3.0 eV, the use of $U_{eff} = 0.0$ or 6.6 eV, underestimate or overestimate the V-O(1) bond stability. Inspection of the figure 5 for the bulk show common features of the O(1)p_z and Vd_{z^2} orbitals for the values of U_{eff} studied, although not so clear as for the surface. Also, there is a shift towards lower energies as U_{eff} increases. As for the surface, the use of $U_{eff} = 6.6$ or 0.0 eV, overestimate or underestimate the V-O(1) bond stability.

V-O(2) and V-O(3) bonds. From figures 4 and 5 for surface and bulk, two comparisons are going to be made looking for common features between orbitals. Atomic projected PDOS of O(2)p_x and V$d_{x^2-y^2}$ orbitals show a small band between −2.2 and −3.2 eV (this small band is also present in the O(1)p_z and Vd_z^2) and the main peak around −4 eV. These features do not depend strongly on the value assigned to U_{eff} and probably the stability of the V-O(2) bond is not correlated with U_{eff}. Atomic projected PDOS of O(3)p_x and O(3)p_y orbitals are compared with the V$d_{x^2-y^2}$ orbital. They, also, show a small peak around −4 eV. The atomic projected DOS of O(3)p_y shows a main peak around −4.5 eV, O(3)p_x and V$d_{x^2-y^2}$ orbitals show a small feature at the same energy. These features do not depend strongly on the value assigned to U_{eff} and probably the stability of the V-O(3) bond is not correlated with U_{eff}, either.

3.3. Charge density distribution in the vanadium-oxygen bonds of the V_2O_5(001) surface

Figure 6 shows the calculated density of electronic charge (e/Bohr^3) distribution around the V-O(1)-O(2)-O(3) atoms in the *xz* plane for U_{eff} values: 0.0, 3.0 and 6.6 eV (left, central and right panels, respectively). In these (nine) charge density diagrams the maximum correspond to 1.19 e Bohr^{-3} and is around the oxygen atoms.

In the top three panels, the minimum electronic charge density shown is 0.16 e Bohr^{-3}. For $U_{eff} = 0.0$ eV there is a discontinuity in this charge density contour between the V and O(1) atoms, due to the absence of charge density larger than 0.16 e Bohr^{-3}. For $U_{eff} = 3.0$ and 6.6 eV the charge density contour is continuous and is thicker for $U_{eff} = 6.6$ eV than for $U_{eff} = 3.0$ eV. This is because larger charge density contours are present for $U_{eff} = 6.6$ eV than for $U_{eff} = 3.0$ eV between the V and O(1) atoms. In this way, the charge accumulation between the V and O(1) atoms is larger for $U_{eff} = 6.6$ eV and smaller for $U_{eff} = 0.0$ eV. Assuming that the near correct value for U_{eff} is 3.0 eV, the electronic charge between the V and O(1) atoms, i. e. in the V-O(1) bond, is under and overestimated, for $U_{eff} = 0.0$ and 6.6 eV, respectively.

For the minimum charge density ploted of 0.10 e Bohr^{-3}, the charge density distribution between the V and O(2) atoms shows that the charge accumulation in the V-O(2) bond is almost not correlated with the value of U_{eff}. For the minimum charge ploted of 0.07 e Bohr^{-3}, the bottom three panels show that the charge density distribution between the V and O(3) seems to be slightly correlated with U_{eff}.

We compare the strength of the three bonds for every U_{eff} value. For $U_{eff} = 3.0$ eV (valid for $U_{eff} = 0.0$ and 6.6 eV as well), following the ideas exposed a few lines above, from figure 6, the upper panel shows there are more charge density contours corresponding to larger than 0.16 e Bohr^{-3} charge density between the V and the O(1) atoms. But there is a lack of these charge density contours between V and O(2), and also between V and O(3). This indicates that there is a larger accumulation of charge in the V-O(1) bond than in the other two V-O bonds. In consecuence, the V-O(1) bond is stronger than the other two V-O bonds. The central panel shows there are charge density contours larger than 0.10 e Bohr^{-3} in the V-O(2) bond but they are not present in the V-O(3) bond. Consecuently, it seems that the strength of the V-O bonds is V-O(1) bond is stronger than V-O(2) bond and this is stronger than V-O(3) bond. This conclusion seems to be supported by the bottom panel, charge contour 0.07 e Bohr^{-3}, in which the accumulation of charge seems to be larger between the V-O(1) than between the V-O(2) and V-O(3). The charge density between V and O(3) in the (near) *y* direction (not shown) seems to be higher than in the *x* but still not higher than in the V-O(2) bond. So, the V-O(3) bond in the *y* is stronger than in the *x* direction but weaker than the V-O(2) bond.

4. Conclusions

A number of density functional theory (DFT(PW91)+U) calculations were performed to calculate the surface lattice parameters (*a* and *b*) of the V_2O_5(001) surface and the V_2O_5 bulk lattice parameters (*a*, *b* and *c*). $U_{eff} = 0.0$ (GGA), 3.0 and 6.6 eV were used. It seems that there is not correlation between the calculated lattice parameters and the value assigned to U_{eff}. This is, there is not a clear evidence that one of these values is the most adequate to describe the experimental results; there is a good agreement between the calculated lattice parameters and the experimental results.

DFT+U was, then, applied to the study of the electronic structure of the systems under investigation. The width of the valence band is not strongly correlated on the value of U_{eff}, it is about 4.87, 4.75 and 4.78 eV for $U_{eff} = 0.0$, 3.0 and 6.6 eV, respectively, for the surface. The calculated energy gap between the valence and the conduction bands shows correlation with the chosen values for U_{eff}: $\approx$ 1.81, 2.19 and 2.95 eV for U_{eff} 0.0, 3.0 and 6.6 eV, respectively. $U_{eff} = 3.0$ eV seems to be the most adequate value to describe the V_2O_5 bulk and its (001) surface following the comparison of the calculated energy gap with the experimental results. The V-O(1) bond stability seems to be under and over estimated for $U_{eff} = 0.0$ and 6.6 eV. The stability of the V-O(2) and V-O(3) bonds does not seem to be strongly correlated with the election of the U_{eff}. According to the calculated charge distribution, for any of the used U_{eff} values, the V-O(1) bond is stronger than the V-O(2) bond and this is stronger than the V-O(3) bonds. It seems that the energy gap between the valence and the conduction bands is strongly correlated with the charge density distribution in the V-O(1) bond, mainly.

Acknowledgment

This work has been supported by Consejo de Investigaciones Científicas y Técnicas (CONICET), Argentina.

References

[1] Haber J 2009 *Catal. Today* **142** 100
[2] Centi G, Cavani F and Trifiro F 2001 *Selective Oxidation by Heterogeneous Catalysis* (New York: Kluwer Academic)
[3] Olive-Méndez S F, Santillán-Rodríguez C R, Campos-Venegas K, Matutes-Aquino J A and Espinosa-Magaña F 2015 *Ceram. Int.* **41B** 6802
[4] Senthil Kumara E, Bellarminea F, Ramanjaneyulua M, Divya Deepthia M S and Rao R 2015 *Scr. Mater.* **108** 48
[5] Kim T, Shin J, Tae-Soo You H, Lee J and Kim J 2015 *Electrochim. Acta* **164** 227
[6] Kovendhan M *et al* 2015 *Current Applied Physics* **15** 622
[7] Aslam M, Ismail I M I, Salah N, Chandrasekaran S, Qamar M T and Hameed A 2015 *Journal of Hazardous Materials* **286** 127
[8] Jin W, Yan S, An L, Chen W, Yang S, Zhao C and Dai Y 2015 *Sensors and Actuators B: Chemical* **206** 284
[9] Vukjović M, Pašti I, Stojković Simatović I, Šljukić B, Milenković M and Mentus S 2015 *Electrochimia Acta.* **176** 130–40
[10] Weckhuysen B M and Keller D E 2003 *Catal. Today* **78** 25
[11] Dunn J P, Koppula P R, Stenger H G and Wachs I E 1998 *Appl. Catal.* B **19** 103
[12] Dunn J P, Stenger H G and Wachs I E 1999 *Catal. Today* **51** 301
[13] Dunn J P, Stenger H G and Wachs I E 1999 *J. Catal.* **181** 233
[14] Cavani F and Trifiro F 1997 *Catal. Today* **36** 431
[15] Gruber M and Hermann K 2013 *J. Chem. Phys.* **138** 094704
[16] Deo G and Wachs I E 1994 *J. Catal.* **146** 323
[17] Wachs I E and Weckhuysen B M 1997 *Appl. Catal.* A **157** 67
[18] Monaci R, Rombi E, Solinas V, Sorrentino A, Santacesaria E and Colon G 2001 *Appl. Catal.* A **214** 203
[19] Koivikko N, Laitinen T, Ojala S, Pitkäaho S, Kucherov A and Keiski R L 2011 *Appl. Catal.* B **103** 72
[20] Wachs I E 2011 *Appl. Catal.* A **391** 36
[21] Kim T and Wachs I E 2008 *J. Catal.* **255** 197

[22] Blasco T, López Nieto J M, Dejoz A and Vázquez M I 1995 *J. of Catal.* **157** 271
[23] Huang B, Huang R, Jin D and Ye D 2007 *Catal. Today* **126** 279
[24] Hu X, Li C and Yang C 2015 *Chemical Engineering Research and Design* **94** 105–11
[25] Kawada T, Hinokuma S and Machida M 2015 *Catalysis Today* B **242** 268
[26] Evert V and Hc¨ok K-H 1998 *Phys. Rev.* B **57** 12727
[27] Giakoumelou I, Parvulescu V and Boghosian S 2004 *J. Catal.* **225** 337
[28] Smith R L, Lu W and Rhorer G S 1995 *Surf. Sci.* **322** 293
[29] Smith R L, Rhorer G S, Lee K S, Seo D K and Whangbo M H 1996 *Surf. Sci.* **367** 87–95
[30] Londero E and Schröder E 2011 *Computer Phys. Communications* **182** 1805–9
[31] Da Costa A, Mathieu C, Barbaux Y, Poelman H, Dalmai-Vennik G and Fiermans L 1997 *Surf. Sci.* **370** 339–44
[32] Enjalbert R and Galy J 1986 *Acta Cryst.* C **42** 1467
[33] Ganduglia-Pirovano M V and Sauer J 2004 *Phys. Rev.* B **70** 045422
[34] Goclon J, Grybos R, Witko M and Hafner J 2009 *J. Phys.: Condens. Matter* **21** 095008
[35] Yin X, Fahmi A, Endou A, Misura R, Gunji I, Yamauchi R, Kubo M, Chatterjee A and Miyamoto A 1998 *Appl. Surf. Sci.* **130–32** 539
[36] Braithwaite J S, Catlow C R A, Gale J D and Harding J H 1999 *Chem. Mater.* **11** 1990
[37] Kresse G, Surnev S, Ramsey M G and Netzer F P 2001 *Surf. Sci.* **492** 329
[38] Reeswinkel T, Music D and Schneider J M 2009 *J. Phys.: Condens. Matter* **21** 145404
[39] Xiao Z R and Guo G Y 2009 *J. Chem. Phys.* **130** 214704
[40] Brázdová V, Ganduglia-Pirovano M V and Sauer J 2004 *Phys. Rev.* B **69** 165420
[41] Chakrabarti A, Hermann K, Druzinic R, Witko M, Wagner F and Petersen M 1999 *Phys. Rev.* B **59** 10583
[42] Londero E and Schröder E 2010 *Phys. Rev.* B **82** 054116
[43] Wang L, Maxisch T and Ceder G 2006 *Phys. Rev.* B **73** 195107
[44] Zimmermann R, Steiner P, Claessens R, Reinert F, Hufner S, Blaha P and Dufek P 1999 *J. Phys.: Condens. Matter* **11** 1657
[45] Chain E E 1991 *Appl. Opt.* **30** 2782
[46] Ganduglia-Pirovano M V, Hofma A and Sauer J 2007 *Surf. Sci. Rep.* **62** 219
[47] Blum R-P, Niehus H, Hucho C, Fortrie R, Ganduglia-Pirovano M V, Sauer J, Shaikhutdinov S and Freund H-J 2007 *Phys. Rev. Lett.* **99** 226103
[48] Alexopoulos K, Reyniers M F and Marin G B 2012 *J. Catal.* **289** 127–39
[49] Laubach S, Schmidt P C, Thißen A, Fernandez-Madrigal F J, Wu Q H, Jaegermann W, Klemm M and Horn S 2007 *PCCP* **9** 2564
[50] Popović Z S and Vukajlović F R 1999 *Phys. Rev.* B **59** 5333
[51] Kresse G and Hafner J 1994 *Phys. Rev.* B **49** 14251
[52] Kresse G and Furthmuller J 1996 *Phys. Rev.* B **54** 11169–86
[53] Blöchl P 1994 *Phys. Rev.* B **50** 17953
[54] Kresse G and Joubert J 1999 *Phys. Rev.* B **59** 1758
[55] Perdew J P, Chevary J A, Vosko S H, Jackson K A, Pederson M R, Singh D J and Fiolhais C 1992 *Phys. Rev.* B **46** 6671–87
[56] Dudarev S L, Botton G A, Savrasov S Y, Humphreys C J and Sutton A P 1998 *Phys. Rev.* B **57** 1505
[57] Ranea V A, Vicente J L, Mola E E and Mananu R U 1999 *Surf. Sci.* **442** 498–506
[58] Oshio T, Sakai Y, Moriya T and Ehara S 1993 *Scanning Microsc.* **7** 33
[59] Poelman H, Vennik J and Dalmai G 1987 *J. Electron Spectrosc. Relat. Phenom.* **44** 251
[60] Zhang Z and Henrich V E 1994 *Surf. Sci.* **321** 133
[61] Lambrecht W, Djafari-Rouhani B and Vennik J 1983 *Surf. Sci.* **126** 558–64
[62] Shin S, Suga S, Taniguchi M, Fuhisawa M, Kanzaki H, Fujimori A, Daimon H, Ueda Y, Kosuge K and Kachi S 1990 *Phys. Rev.* B **41** 4993
[63] Kokalj A 2003 *Comp. Mater. Sci.* **28** 155
[64] Wyckoff R W G 1965 *Crystal Structures Interscience* 2nd edn (New York: Wiley)
[65] Momma K and Izumi F 2011 VESTA 3 for three-dimensional visualization of crystal, volumetric and morphology data *J. Appl. Crystallogr.* **44** 1272–6